Periodico di Mineralogia (2012), 81, 2, 237-256 DOI: 10.2451/2012PM00014

PERIODICO di MINERALOGIA
established in 1930

An International Journal of
MINERALOGY, CRYSTALLOGRAPHY, GEOCHEMISTRY,
ORE DEPOSITS, PETROLOGY, VOLCANOLOGY
and applied topics on *Environment*, *Archeometry* and *Cultural Heritage*

Chromian spinels and magnetite of serpentinites, steatitic rocks, tremolite asbestos and chloritites from Bragança massif, northeastern Portugal

Rui José dos Santos Teixeira[1,*], Ana Margarida Ribeiro Neiva[2] and Maria Elisa Preto Gomes[1]

[1]Department of Geology, University of Trás-os-Montes e Alto Douro,
5001-801 Vila Real and Geosciences Centre, University of Coimbra, Portugal
[2]Department of Earth Sciences, University of Coimbra,
3000-272 Coimbra and Geosciences Centre, University of Coimbra, Portugal
[*]Corresponding author: *rteixeir@utad.pt*

Abstract

At Bragança region, northeastern Portugal, accessory chromian spinels and magnetite occur in serpentinites and steatitic rocks and rarely in tremolite asbestos and chloritites. The chromian spinels have a large range in composition, which is related to serpentinization and other subsequent alteration processes such as steatization. Four varieties of zoned chromian spinels were distinguished: 1- zoned crystals with a Cr-rich hercynite core and a ferrian chromite rim in serpentinite from Donai; 2- zoned crystals with an aluminian chromite core and a ferrian chromite rim in steatitic rock from Donai; 3- zoned aluminian chromite crystals showing a rim richer in Fe^{2+} and poorer in Mg than the core, found in Donai tremolite asbestos; 4- zoned chromian magnetite crystals showing a rim richer in Fe^{3+} and poorer in Cr than the core, in serpentinites and steatitic rocks from Sete Fontes and Soeira/Pena Maquieira. Unzoned aluminian chromite crystals were found in Donai chloritite. Magnetite from the Donai serpentinite and steatitic rocks from Sete Fontes and Soeira/Pena Maquieira has a composition close to the ideal formula.

Key words: chromian spinels; ferrian chromite; magnetite; crystal zoning; Bragança massif; Portugal.

Introduction

Accessory chromian spinels occurring in ultramafic and mafic rocks are frequently altered (Burkhard, 1993). The alteration is usually attributed to serpentinization and steatization processes which commonly produce ferrian chromite at borders or along cracks of chromian spinel grains (e.g., Wylie et al., 1987; Burkhard, 1993; Peltonen, 1995; Proenza et al., 1999; Pooley, 2004; Mellini et al., 2005; Karipi et al., 2007; Khalil and El-Makky, 2009). According to

Barnes (2000) and González-Jiménez et al. (2009), the alteration of chromian spinels during metamorphism mainly depends on the chemical and mineralogical composition of the host protolith (anhydrous versus serpentinised), the degree of metamorphism (pressure and temperature), the timing of prograde and/or retrograde evolution and the nature of metamorphic fluids. Solid state alteration (Beeson and Jackson, 1969; Shen et al., 1988; Burkhard, 1993; Angeli et al., 2001) and overgrowth (Ulmer, 1974) are considered the main mechanisms responsible by the formation of ferrian chromite. Solid state alteration may be caused either by the outward diffusion of Mg and Al to areas having a high activity of Si (Beeson and Jackson, 1969; Shen et al., 1988; Leblanc and Nicolas, 1992) or by the infiltration and replacement/dissolution through the rims of Mg, Al and Cr during low-grade alteration processes, such as serpentinization or steatization (Burkhard, 1993; Angeli et al., 2001; Mellini et al., 2005; Garuti et al., 2007; Karipi et al. 2007; Sansone et al., 2012). However, Angeli et al. (2001) and Izquierdo et al. (2002) also considered diffusion as an important alteration mechanism of Cr-rich spinels during medium-grade metamorphism conditions. Furthermore, the dissolution of Cr is favoured in a reducing environment, whereas reprecipitation of Cr occurs under locally oxidizing conditions (e.g., Ulmer, 1974; Burkhard, 1993).

The compositional variation of ferrian chromite can be explained by: a) intergrowths of oxides other than those having the spinel structure in a submicrometric scale (Shen et al., 1988); b) solid solutions of different spinels (Shen et al., 1988); c) both solid solutions and mixtures of oxides (Shen et al., 1988); d) nanometric associations of chromian magnetite, chlorite and lizardite (Mellini et al., 2005); e) two intimately intermixed spinel phases (Garuti et al., 2007). Thus, the ferrian chromite rims differ significantly from their Cr-rich spinel cores in their chemical composition and physical properties including their higher reflectance and lower hardness (Burkhard, 1993; Garuti et al., 2007).

After main serpentinization episodes, some chromian spinel grains can also become surrounded by chlorite aureoles (e.g., Pinsent and Hirst; 1977; Gianfagna et al., 1992; O' Hanley, 1996; Mellini et al., 2005; Garuti et al., 2007; González-Jiménez et al., 2009), which depends on the local abundance of Cr, Al and Mg and, ultimately, on the chromian spinel composition. According to Mellini et al. (2005), the chemical changes would reflect the hydrothermal metamorphic reactions between magmatic chromian spinels and surrounding post-serpentinization silicate matrix. Consequently, the Al diffuses out of magmatic chromian spinel leaving behind a (Fe, Cr)-rich spinel and promoting the formation of chlorite aureoles.

This paper reports the occurrence, chemical compositions and zoning of accessory chromian spinels and magnetite in serpentinites, steatitic rocks, tremolite asbestos and chloritites from several areas in the northern ophiolitic terrane in the Bragança massif in order to compare the compositions of chromian spinels, produced by different alteration processes.

Geological setting

Accessory spinels occur in serpentinites and steatitic rocks and rarely in tremolite asbestos and chloritites in the Bragança Nappe Complex, in northeastern Portugal. This complex consists of four main thrust sheets (Figure 1), separated by three major overthrusts (Ribeiro et al., 1990). They are, from bottom to top: 1) a parautochthonous thrust complex formed mainly of Silurian metasediments (phyllites, graywackes and quartzites) overlain by Lower Devonian flysch at chlorite schist metamorphic facies; 2) a lower allochthonous thrust complex consisting of Silurian metasedimentary formations which include alkaline basalts and peralkaline rhyolites

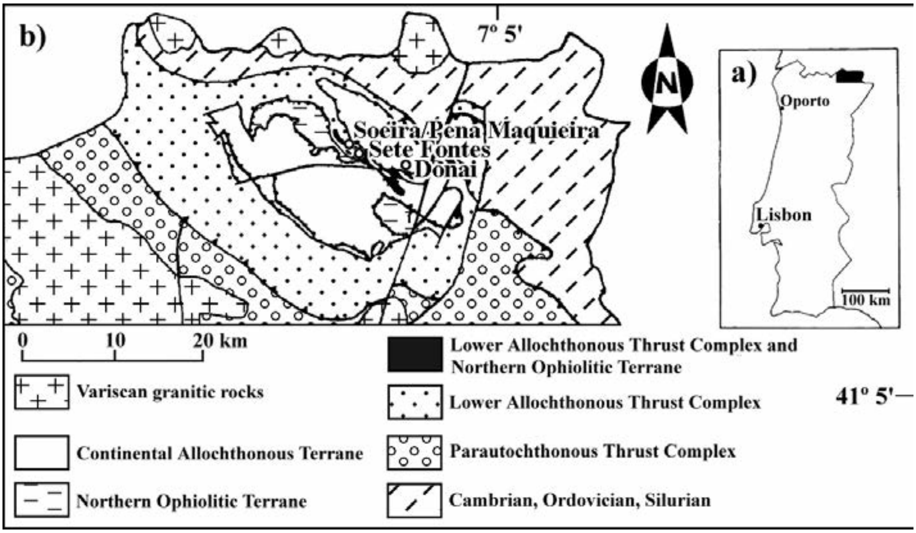

Figure 1. a) Index map of the areas studied. b) Geological map of Bragança Nappe Complex (modified from Ribeiro, 1974).

formed by continental rifting and some relicts of mineral parageneses from the high-pressure Variscan metamorphism (Munhá et al., 1984); 3) a northern ophiolitic terrane, comprising sequences of an early prograde amphibolite facies of Variscan metamorphism dismembered by the Variscan orogeny; 4) a continental allochthonous terrane, consisting mostly of granulites, mafic and ultramafic igneous rocks and paragneisses which enclose eclogite boudins (Bridges et al., 1993; Marques et al., 1996). The two last allochthons correspond to the so-called Bragança massif, which outcrops above the lower allochthonous thrust complex. The spinels studied are from the northern ophiolitic terrane (Figure 1).

At Donai (Figure 2), serpentinites are intercalated within Lower Devonian chlorite phyllites along a N80ºW shear zone (Meireles et al., 1999). Slip-fibre asbestos veins occur along shear zones and faults cutting serpentinites, but mass-fibre asbestos also occurs as intercalations associated with amphibole schists and rarely with chloritites. Talc schist was also found associated with serpentinites.

At Sete Fontes (Figure 3), a tabular Silurian-Devonian steatitic rock is in contact with serpentinites belonging to the northern ophiolitic terrane at the hanging wall and quartz-phyllites and phyllites at the footwall. The steatitic rock contains intercalations of chloritites and serpentinites.

At Soeira (Figure 4), a steatitic rock is overlain at South by mafic granulites, retro-metamorphosed to amphibolite facies, belonging to the continental allochthonous terrane, while at North there is progressive steatization of serpentinites. The steatitic rock at Pena Maquieira has been folded to an antiform where two parts can be distinguished (Figure 5): a) the eastern part consists of a elongated steatitic rock with NW-SE trend of; b) the southern part is formed by several outcrops of steatitic rock within serpentinites, which show gradual contacts to the steatitic rock (Cotelo Neiva, 1948; Vilela de Matos et al., 1990; Teixeira, 2000).

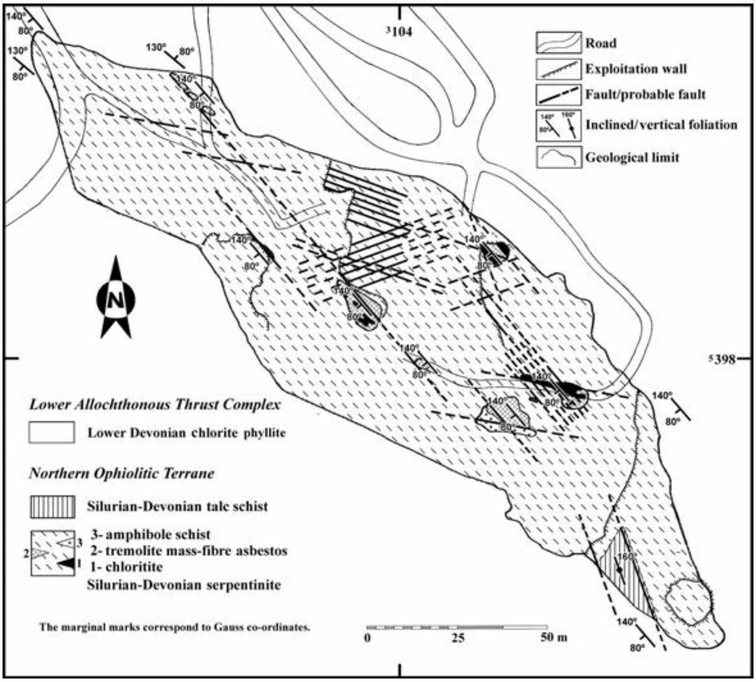

Figure 2. Geological map of the outcrop at Donai. Geological mapping by Teixeira (2000).

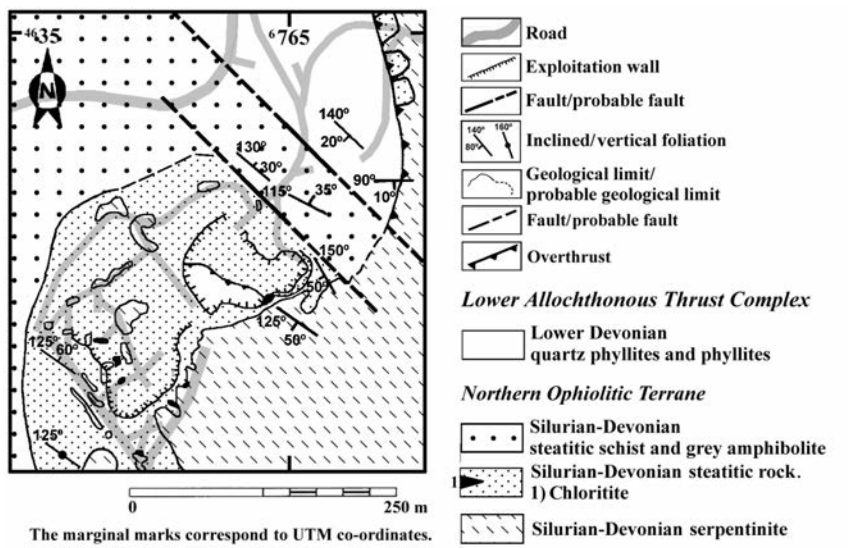

Figure 3. Geological map of Sete Fontes mine. Geological mapping by Vilela de Matos et al. (1990), reviewed by Teixeira (2000).

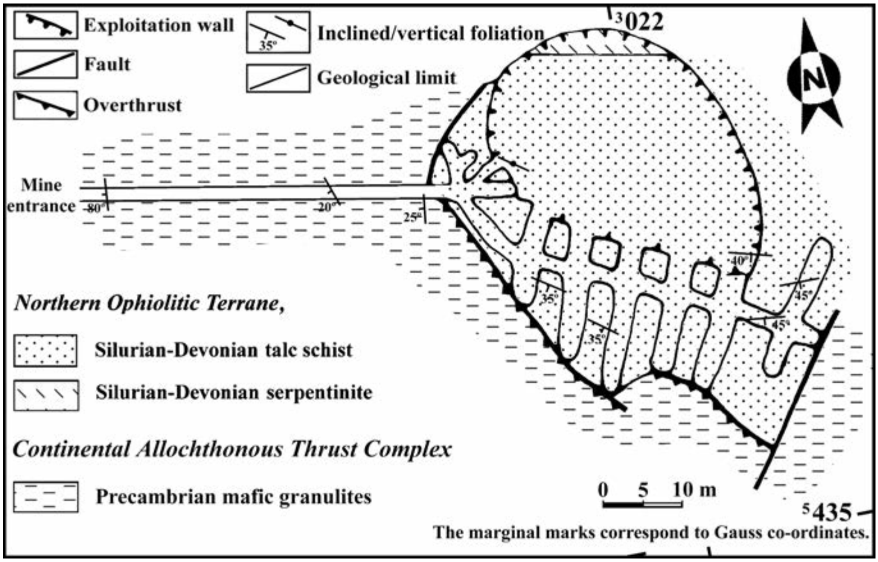

Figure 4. Geological map of Soeira mine. Geological mapping by Ramos et al. (1989).

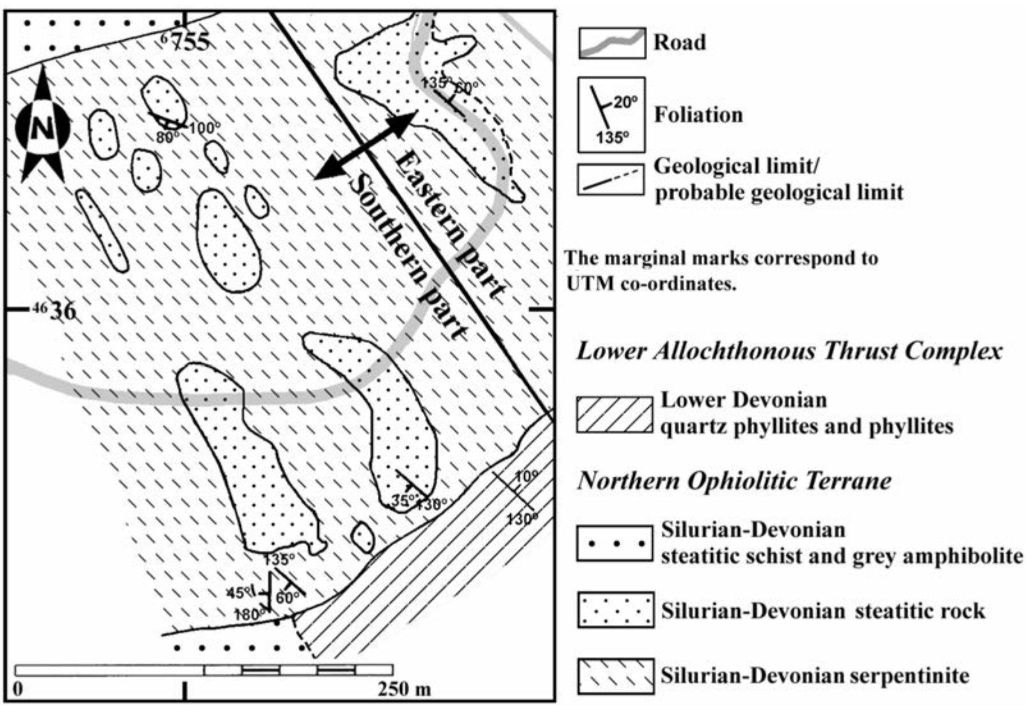

Figure 5. Geological map of Pena Maquieira area. Geological mapping by Vilela de Matos et al. (1990).

Petrography

The serpentinites from Donai contain olivine megacrysts, whereas those from Sete Fontes and Soeira/Pena Maquieira are texturally homogeneous. γ-serpentine (antigorite) interpenetrating textures were commonly recognised, but α-serpentine (lizardite) mesh and hourglass textures after olivine and pyroxene bastites were also found in Donai and Soeira serpentinite. The serpentinites consist of antigorite (> 90 %), lizardite, talc, chlorite, chromian spinel, magnetite, pentlandite, breunnerite and dolomite (Figure 6). However, at Donai pyrrhotite (Figure 6) and tremolite are also found and olivine megacrysts are locally replaced by lizardite and products of alteration with intermediate optical properties between those of olivine and lizardite. Soeira serpentinite also contains lizardite (Teixeira, 2000). Locally, chromian spinels are surrounded by chlorite aureoles, which under crossed nicols show brown to deep-blue anomalous birefringence (Figure 6c). Generally, these chlorite aureoles seem to overgrow the serpentine textures, but locally there are also some optical evidences of a serpentine/chlorite intergrown.

At Donai and Soeira, two types of steatitic rocks are distinguished: a) foliated talc schists and b) steatites with randomly orientated platy crystals. At Sete Fontes and Pena Maquieira steatites dominate and consist of more than 70 % of talc, which occurs in aggregates of platy crystals (smaller than 100 μm x 50 μm), frequently intergrown with chlorite. They also contain breunnerite and dolomite, which locally reach 25 %. The talc matrix and carbonates generally contain abundant inclusions of chromian spinel, magnetite, pentlandite, millerite, siegenite and pyrite (Figure 7). However, at Sete Fontes they also contain ilmenite inclusions.

At Donai, there is tremolite asbestos which commonly consist of slip-fibre veins (with the fibre axis sub-parallel to vein walls) and mass-fibre veins (with randomly orientated fibres) and rarely of cross-fibre veins with fibre axis normal to vein walls. Chromian spinel crystals were found in the mass-fibre asbestos. In these asbestos, secondary clinochlore and talc fill fractures of tremolite, but clinochlore was also found in aggregates surrounding single anhedral chromian spinel crystals or in small ellipsoidal nodules.

The chloritite from Donai is mainly composed of clinochlore, but it also contains single anhedral crystals of ilmenite and chromian spinel.

Occurrence of spinels in serpentinites, steatitic rocks, tremolite asbestos and chloritites from Bragança Massif

Chromium-rich hercynite, aluminian chromite, ferrian chromite, chromian magnetite and magnetite of end-member composition were found in serpentinites, steatitic rocks, tremolite asbestos and chloritites from Bragança Massif (Figures 6, 7 and 8).

The chromian spinel in the serpentinites occurs as anhedral single crystals, which are up to 500 μm x 300 μm. Backscattered electron images and also reflected-light microscopy show two different types of zoned chromian spinels with: a) a Cr-rich hercynite core and a ferrian chromite rim at Donai (Figure 6a); b) chromian magnetite crystals with a rim richer in Fe^{3+} and poorer in Cr than the core at Sete Fontes and Soeira/Pena Maquieira (Figure 6b). Locally, the Cr-rich hercynite crystals are surrounded by chlorite (Figure 6c). In general, magnetite occurs as anhedral crystals in the rims of the mesh cells (Figure 6d) and rarely as discrete crystals in mesh centres. However, magnetite may also occur as fine-grained crystals scattered in antigorite interpenetrating textures and included in carbonates and talc or rarely as single coarser grains, up to 70 μm x 35 μm. Aggregates of magnetite + pyrrhotite + pentlandite were also found in Donai serpentinite (Figure 6e).

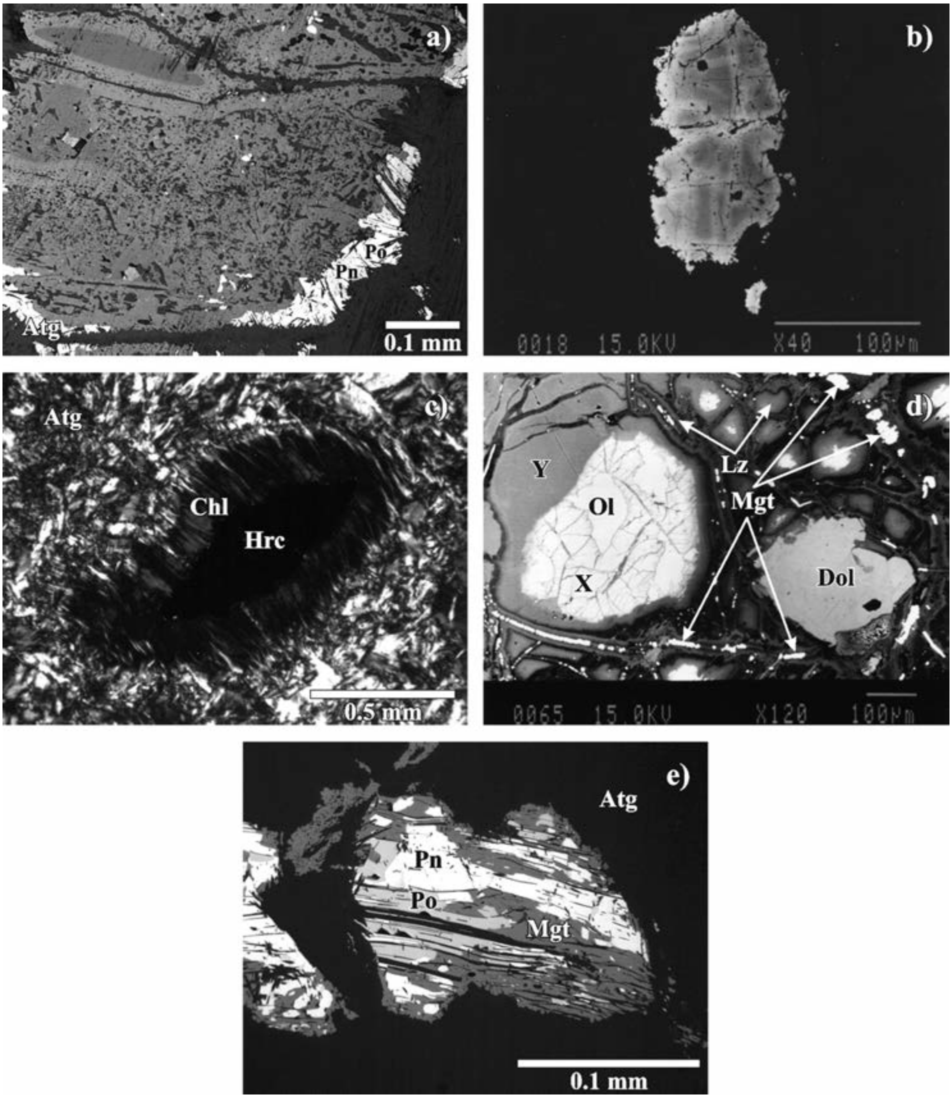

Figure 6. Photomicrographs of serpentinites from Donai and Soeira/Pena Maquieira: a) single zoned crystal with a dark grey Cr-rich hercynite core and a light grey ferrian chromite rim, surrounded by sulphides (Po- pyrrotite, Pn- pentlandite) from Donai serpentinite (reflected-light microscopy); b) backscattered electron image of a single zoned chromian magnetite crystal showing a dark grey core and a light grey rim and light grey areas along the cracks from Soeira/Pena Maquieira serpentinite; c) single crystal of Cr-rich hercynite (Hrc) surrounded by a rim of chlorite (Chl) from Donai serpentinite (crossed nicols); d) backscattered electron image of mesh texture, showing the centre of olivine (Ol) and products of alteration with intermediate optical properties between those of olivine and lizardite (X, Y) and mesh rim of lizardite (Lz) from Donai serpentinite; Mgt- magnetite, Dol- dolomite; e) aggregate of magnetite (Mgt) + pyrrhotite (Po) + pentlandite (Pn) in Donai serpentinite; Atg- antigorite (reflected-light microscopy).

The steatitic rocks contain anhedral crystals of chromian spinel up to 500 μm x 200 μm. Two different zoned chromian spinels were distinguished: a) at Donai, with an aluminian chromite core and a ferrian chromite rim (Figure 7a); b) at Sete Fontes and Soeira/Pena Maquieira, chromian magnetite crystals with a diameter greater than 150 μm usually show a sharp boundary between an homogeneous core and an porous rim (Figure 7b), but if the diameter is smaller they only present a cryptic zoning. In general, the magnetite is subhedral and occurs as single crystals, which are commonly smaller than 100 μm x 35 μm.

The aluminian chromite from Donai tremolite asbestos is zoned showing a variation in reflectance from the core to the rim (Figure 7c) and in crossed nicols the core is red in colour, while the rim is opaque.

Rare aluminian chromite crystals were found in Donai chloritite. They are always anhedral and optically unzoned.

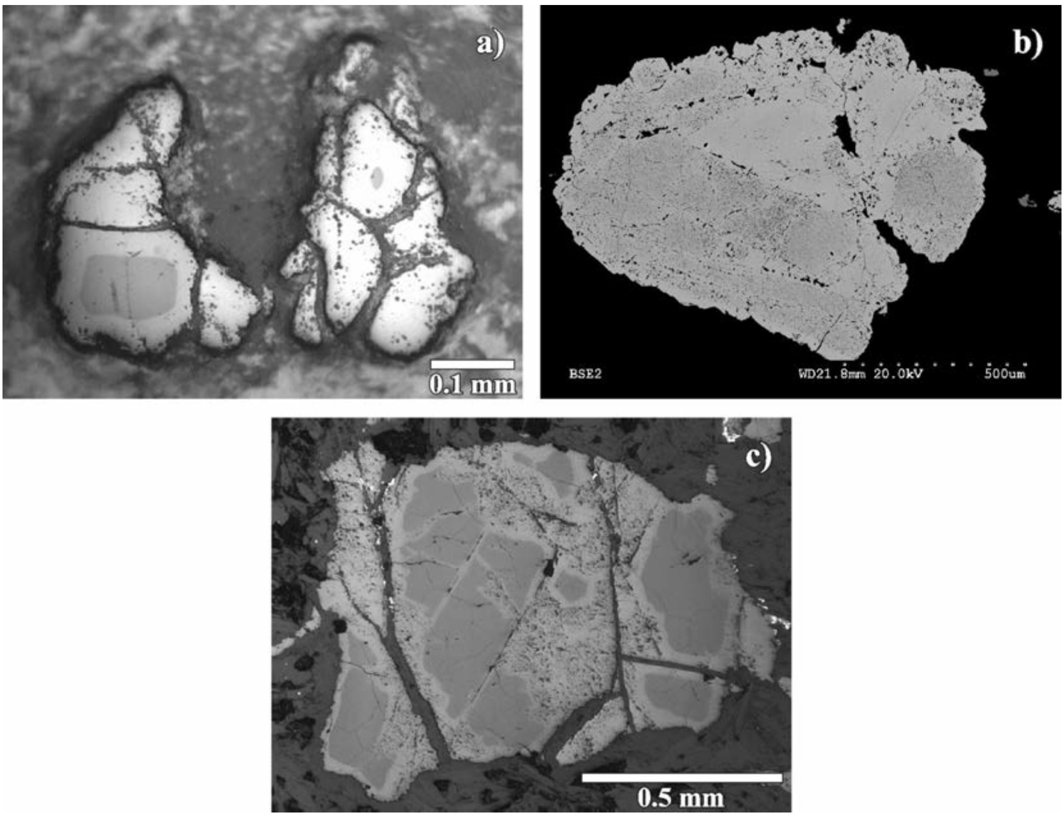

Figure 7. Photomicrographs of steatitic rocks from Donai and Sete Fontes and tremolite asbestos from Donai: a) zoned crystals with a dark grey aluminian chromite core and a light grey ferrian chromite rim from Donai steatitic rock (reflected-light microscopy); b) scanning electron microscope image of a chromian magnetite crystal showing a chemically and optically homogeneous core and an heterogeneous rim with pores refilled by talc from Sete Fontes steatite, probably formed under highly oxidizing conditions; c) zoned single crystal of aluminian chromite showing a dark grey core and a light grey rim and areas along the cracks from Donai tremolite asbestos.

In general, the rims and areas along fractures of all chromian spinel crystals have a spongy texture due to the presence of pores, usually refilled with serpentine, talc or carbonates, while the cores are homogeneous (Figures 6a, b and 7a, b, c).

Experimental

Chromian spinels and magnetite were analysed on a Cameca Camebax electron microprobe at the Laboratório Nacional de Energia e Geologia, São Mamede de Infesta, Portugal. Analyses were conducted at an accelerating voltage of 15 kV and a beam current of 20 nA. Standards used include wollastonite (Si) and (Ca), $MnTiO_3$ (Ti) and (Mn), Al_2O_3 (Al), Cr_2O_3 (Cr), Fe_2O_3 (Fe), MgO (Mg), sphalerite (Zn), NiO (Ni) and CoO (Co). Each element was counted for 20 s at the peak and 10 s at the background. ZAF corrections were applied. A JEOL JXA 8600 electron microprobe of the Department of Earth Sciences, University of Bristol, United Kingdom, was used to obtain images of chromian spinels.

Results

The spinel crystals were analysed by electron microprobe and the compositions are given in Tables 1, 2, 3 and 4.

In serpentinite and steatitic rock from Donai, the single zoned spinel crystals have a ferrian chromite rim richer in Fe^{3+}, Ti, Fe^{2+}, Cr/(Cr + Al) and poorer in Al, Mg, Co and Mg/(Mg + Fe^{2+}) than the respective core, which is of Cr-rich hercynite in serpentinite and aluminian chromite in steatitic rock (Table 1, Figures 8a, 9). In Donai tremolite asbestos, zoned crystals were found with a core and a rim of aluminian chromite, but Mg decreases and Fe^{2+} increases from core to rim (Table 1). The unzoned aluminian chromite crystals of Donai chloritite are the richest in Zn (Table 1).

At Sete Fontes and Soeira/Pena Maquieira, single zoned crystals of chromian magnetite were found in serpentinites and steatitic rocks (Figures 8b, c). Those with a diameter greater than 150 μm have generally a rim richer in Fe^{3+}, Fe^{2+} and Ni and poorer in Al, Cr, Ti, Mg, and Zn than the respective core (Table 2, Figures 10a, b). If the diameter of those single zoned crystals is smaller than 150 mm, the rim is richer in Fe^{3+} and poorer in Cr than the core (Table 3, Figure 10b), and the rim of the smallest crystals (with a diameter smaller than 100 μm) is the richest in Fe^{3+} and the poorest in Cr (Table 3, Figure 10b).

Magnetite from Donai serpentinite and steatitic rocks from Sete Fontes and Soeira/Pena Maquieira has a composition close to the ideal formula, but a small amount of Cr replaces Fe^{3+}, small contents of Mg, Ni, Mn and Ca replace Fe^{2+} and also some Ti enters the magnetite structure (Table 4).

Discussion

At Donai, serpentinization is the most important alteration, but steatization, chloritisation and asbestisation also took place. The single zoned spinel crystals have a Cr-rich hercynite core in serpentinites and an aluminian chromite core in steatitic rocks and always a ferrian chromite rim, defining a trend of increase in Fe^{3+} and decrease and Al from core to rim (Figure 8a, and trend A in Figure 11a). The compositional boundary between core and rim is usually sharp (Figures 6a, b). The decrease in Al towards the grain rim is balanced by a concomitant increase of Fe^{3+} and Ti (Figures 9a, c), while the increasing Fe^{2+} content toward the rim is balanced by a sympathetically decrease in Mg (Figure 9b) and Co (Table 1). Such compositional trend is similar to that of alteration of aluminian chromite to ferrian chromite (e.g., Burkhard, 1993; Peltonen, 1995; Mellini et al., 2005; Garuti et al., 2007; Khalil and El-Makky, 2009). Since there are no significant increase in Cr from core to rim, the compositional trend A

Table 1. Electron microprobe analyses of Cr-rich hercynite, aluminian chromite and ferrian chromite in serpentinites, steatitic rocks, tremolite asbestos and chloritites from Donai.

	Serpentinite		Steatitic rock		Tremolite asbestos		Chloritite
	a	b	c	b	c	c	c
	Core	Rim	Core	Rim	Core	Rim	
SiO_2	0.04	0.09	0.02	0.04	0.02	0.03	0.04
TiO_2	0.01	2.57	0.05	3.12	0.02	0.06	0.08
Al_2O_3	27.45	6.32	24.40	4.41	21.60	21.30	21.92
Cr_2O_3	38.07	34.89	38.60	34.31	42.63	41.68	42.07
Fe_2O_3	1.89	20.66	4.29	23.08	3.78	3.52	1.02
FeO	23.04	31.48	25.81	32.57	27.58	31.12	27.96
MgO	8.13	1.55	5.51	1.07	5.37	2.98	2.33
ZnO	0.67	0.75	2.04	0.97	n. a.	n. a.	4.39
NiO	0.16	0.14	0.04	0.11	n. a.	n. a.	0.04
CoO	0.03	-	0.05	-	n. a.	n. a.	0.01
CaO	0.01	0.02	0.01	-	0.01	0.02	0.02
Total	99.50	98.47	100.82	99.68	101.01	100.71	99.88
Si	0.011	0.025	0.006	0.011	0.006	0.006	0.011
Al	8.094	2.183	7.349	1.529	6.563	6.601	6.884
Cr	7.526	8.081	7.794	7.967	8.684	8.665	8.856
Fe^{3+}	0.355	4.555	0.824	5.102	0.733	0.696	0.205
Ti	0.003	0.565	0.009	0.690	0.005	0.013	0.016
Σ	15.99	15.41	15.98	15.30	15.99	15.98	15.97
Mg	3.028	0.676	2.099	0.466	2.061	1.169	0.925
Fe^{2+}	4.819	7.715	5.514	8.001	5.945	6.844	6.227
Zn	0.123	0.162	0.385	0.210	-	-	0.862
Ni	0.032	0.033	0.008	0.025	-	-	0.008
Co	0.006	-	0.009	-	-	-	0.002
Ca	0.003	0.006	0.003	-	0.003	0.006	0.005
Σ	8.01	8.59	8.02	8.70	8.01	8.02	8.03

a- Cr-rich hercynite; b- ferrian chromite; c- aluminian chromite; Fe_2O_3 and FeO were calculated according to the method of Droop (1987); - : not detected; n. a: not analysed. Number of cations on the basis of 32 atoms of oxygen.
Analyst: R.J.S. Teixeira.

(Figure 11a) shouldn't be attributed to a primary zoning corresponding to magmatic differentiation (e.g., Haggerty, 1976; Burkhard, 1993), but mainly to the effects of the serpentinization and subsequent alteration processes.

The rare unzoned aluminian chromite crystals that occur in Donai chloritite (Table 1) could correspond to small relicts preserved in an igneous protolith compositionally distinct from that of the serpentinites, probably of mafic nature. These aluminian chromite crystals were incompletely altered by the serpentinization fluids, and were stable and unaltered during chloritisation. Donai serpentinite and chloritite were penetrated by tremolite asbestos veins, which contain very rare zoned aluminian

Table 2. Electron microprobe analyses of chromian magnetite crystals with a diameter greater than 150 μm in serpentinites and steatitic rocks from northeastern Portugal.

	Serpentinites				Steatitic rocks			
	Sete Fontes		Soeira/Pena Maquieira		Sete Fontes		Soeira/Pena Maquieira	
	Core	Rim	Core	Rim	Core	Rim	Core	Rim
SiO_2	-	0.04	-	0.03	0.21	0.37	0.03	0.03
TiO_2	0.20	0.09	0.40	0.05	0.28	-	0.25	0.05
Al_2O_3	0.09	0.04	0.09	0.02	0.17	0.04	0.14	0.01
Cr_2O_3	15.31	8.37	23.02	7.45	18.73	6.85	29.27	3.42
Fe_2O_3	53.79	60.97	44.55	61.82	48.51	61.36	38.96	65.87
FeO	30.91	30.88	30.15	30.72	30.62	30.77	30.84	31.02
MnO	-	-	0.27	-	-	-	-	-
MgO	0.26	0.17	0.41	0.09	0.42	0.29	0.22	0.05
ZnO	0.22	0.08	0.28	0.10	0.18	0.23	0.72	0.04
NiO	0.31	0.43	0.30	0.55	0.27	0.28	0.11	0.28
CoO	-	-	0.05	-	-	-	0.01	-
CaO	0.01	-	0.01	0.01	0.01	0.02	0.01	0.02
Total	101.10	101.07	99.53	100.84	99.40	100.21	100.56	100.79
Si	-	0.011	0.002	0.009	0.063	0.114	0.009	0.009
Al	0.032	0.011	0.033	0.007	0.063	0.015	0.051	0.004
Cr	3.654	2.005	5.550	1.792	4.525	1.655	6.976	0.825
Fe^{3+}	12.222	13.918	10.226	14.159	11.158	14.102	8.841	15.126
Ti	0.045	0.022	0.093	0.011	0.064	-	0.058	0.013
Σ	15.95	15.97	15.90	15.98	15.87	15.89	15.94	15.98
Mg	0.114	0.078	0.187	0.042	0.189	0.130	0.100	0.024
Fe^{2+}	7.806	7.834	7.692	7.819	7.827	7.859	7.777	7.917
Zn	0.049	0.016	0.062	0.022	0.040	0.051	0.159	0.008
Ni	0.076	0.104	0.073	0.136	0.066	0.068	0.025	0.069
Co	-	-	0.011	-	-	-	0.002	-
Mn	-	-	0.070	-	-	-	-	-
Ca	0.002	-	0.002	0.004	0.003	0.005	0.002	0.005
Σ	8.05	8.03	8.10	8.02	8.13	8.11	8.07	8.02

Fe_2O_3 and FeO were calculated according to the method of Droop (1987); - : not detected.
Number of cations on the basis of 32 atoms of oxygen.
Analyst: R.J.S. Teixeira.

chromite with a rim poorer in Mg, Mg/(Mg + Fe^{2+}) and richer in Fe^{2+} than the respective core (Table 1, Figures 11a, b). This zoning implies a significant dissolution of Mg (Figure 7c), but there is not any Fe^{3+} enrichment as in serpentinites and steatic rocks from Donai, which may evidence the role of tremolite in the fO_2 buffering (Zakrevskaya et al., 2009).

In general, during steatization of ultramafic rocks from Sete Fontes and Soeira/Pena Maquieira there is the formation of a chromian magnetite rim richer in Fe^{3+}, Fe^{2+}, Ni and poorer in Al, Cr, Ti, Mg, and Zn than the chromian magnetite core (Tables 2, 3 and trend B in Figure

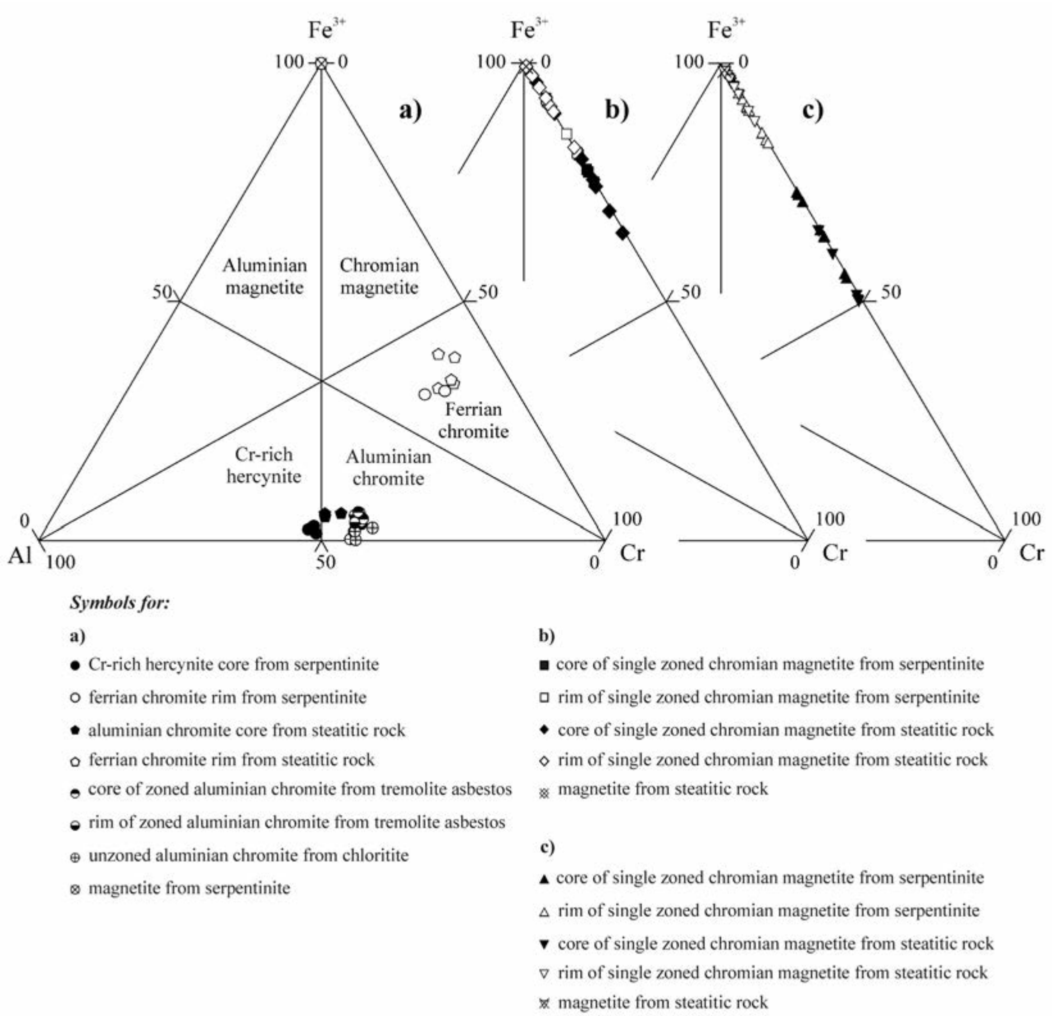

Figure 8. Compositions of spinels from Bragança massif plotted on the Fe^{3+}-Al-Cr ternary diagram (adapted from Stevens, 1944 and Deer et al., 1992). a) Donai. b) Sete Fontes. c) Soeira/Pena Maquieira.

11a). The boundary between rim and core is sharp (Figures 7a, b) if the Cr content of the core is higher than 3.65 a.p.f.u. (crystals with diameter greater than 150 μm; Table 2), but if the Cr content is lower than that value it is only possible to detect a cryptic zoning in crystals with diameter smaller than 150 μm (Table 3). The decrease in Cr, Al and Ti from core to rim is compensated by an increase of Fe^{3+} (Figures 10a, b and Tables 2, 3), while the increasing Fe^{2+} and Ni content toward the rim is balanced by a decrease in Mg and Zn (Tables 2, 3). Furthermore, the investigated chromian magnetite contains negligible amounts of Al_2O_3 (up to 0.17 wt %),

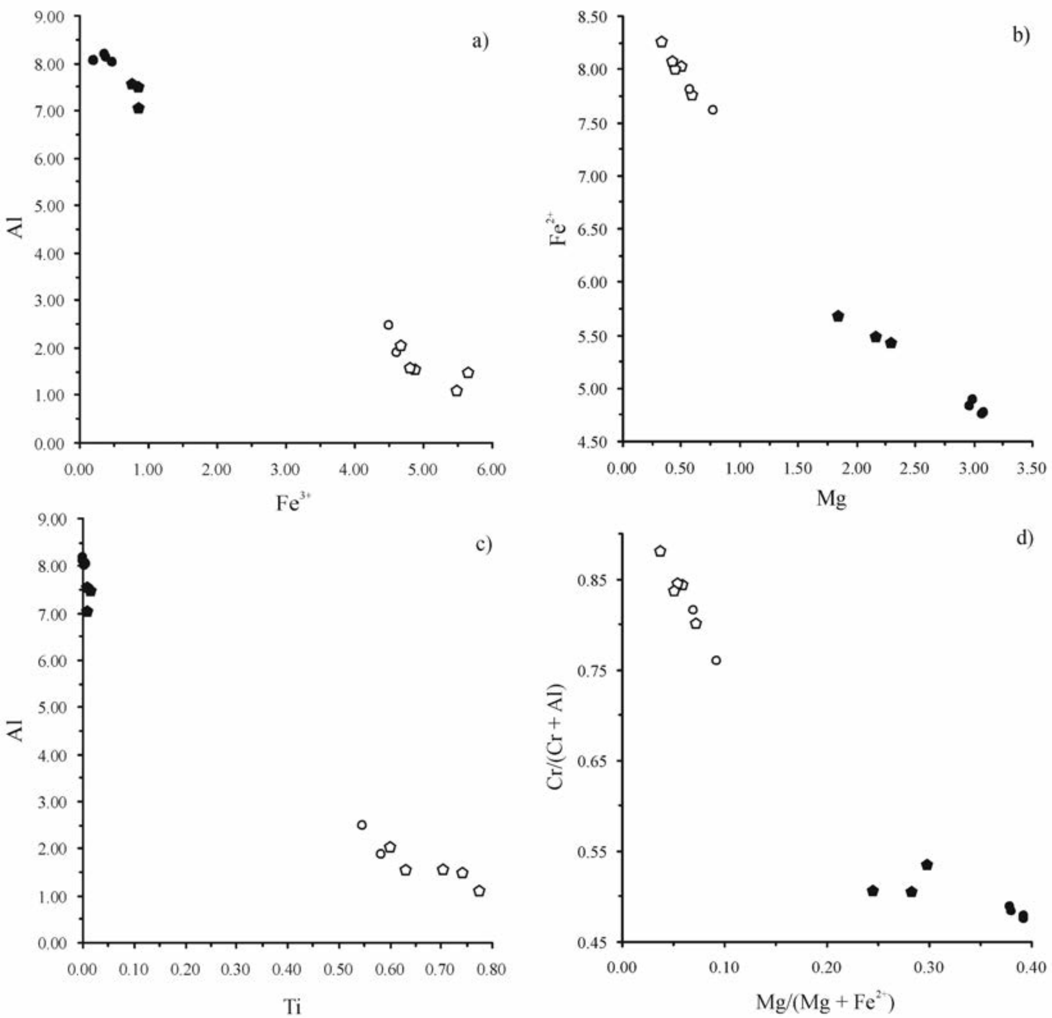

Figure 9. Plots of Cr-rich hercynite, aluminian chromite and ferrian chromite of serpentinite and steatitic rock from Donai. a- Al versus Fe^{3+}; b- Fe^{2+} versus Mg; c- Al versus Ti; d- Cr/(Cr + Al) versus Mg/(Mg + Fe^{2+}). Symbols as in Figure 8a.

confirming its secondary origin, since primary magnetite crystallized from mafic magmas display considerable amounts of Al rather than Cr (Barnes and Roeder, 2001; Mondal et al., 2006).

Therefore, the spongy alteration texture of the rims and areas parallel to cracks of the chromian spinel crystals (Figures 6a, b and 7a, b) can be attributed to the dissolution of several elements, Al, Cr, Ti, Mg, Zn, Co from these crystals (Tables 1, 2 and 3) during the serpentinization and/or steatization processes (Garuti et al., 2007). On the other hand, the chromian spinels from Bragança Massif with Cr/(Cr + Al) lower than 0.60 are usually surrounded by chlorite

Table 3. Electron microprobe analyses of chromian magnetite crystals with a diameter smaller than 150 μm in steatitic rocks from northeastern Portugal.

	Sete Fontes				Soeira/Pena Maquieira	
	Ø > 100 mm		Ø < 100 mm		Ø < 100 mm	
	Core	Rim	Core	Rim	Core	Rim
SiO_2	0.02	0.04	0.05	0.13	0.29	0.09
TiO_2	0.08	0.03	0.01	0.04	0.03	0.03
Al_2O_3	0.01	0.04	0.01	0.01	0.03	0.02
Cr_2O_3	10.10	6.04	3.01	1.64	2.27	1.66
Fe_2O_3	58.57	62.65	66.14	67.53	66.22	67.71
FeO	30.60	30.18	30.05	31.00	30.60	31.13
MgO	0.06	0.09	0.09	0.06	0.31	0.06
ZnO	0.15	0.21	0.07	0.12	0.09	-
NiO	0.32	0.39	0.99	0.33	0.41	0.30
CoO	-	0.02	0.01	-	-	-
CaO	0.14	0.23	0.07	0.01	-	-
Total	100.05	99.92	100.50	100.87	100.25	101.00
Si	0.006	0.013	0.013	0.039	0.088	0.027
Al	0.004	0.011	-	0.004	0.008	0.008
Cr	2.444	1.465	0.728	0.396	0.548	0.399
Fe^{3+}	13.504	14.484	15.240	15.504	15.255	15.527
Ti	0.018	0.008	0.002	0.009	0.008	0.005
Σ	15.98	15.98	15.98	15.95	15.91	15.97
Mg	0.026	0.041	0.039	0.030	0.140	0.026
Fe^{2+}	7.841	7.753	7.696	7.909	7.835	7.934
Zn	0.033	0.048	0.014	0.027	0.018	-
Ni	0.079	0.096	0.245	0.080	0.099	0.073
Co	-	0.005	0.002	-	-	-
Ca	0.046	0.076	0.022	0.002	-	-
Σ	8.03	8.02	8.02	8.05	8.09	8.03

Fe_2O_3 and FeO were calculated according to the method of Droop (1987); - : not detected.
Number of cations on the basis of 32 atoms of oxygen.
Analyst: R.J.S. Teixeira.

aureoles (Figure 6c), while those with Cr/(Cr + Al) greater than 0.95 just show chromian magnetite rims (Figure 11b). Interestingly, in both alteration trends (A and B; Figure 11a) there is a common general tendency of increase in Fe^{3+} and decrease and Al from core to rim of chromian spinels, which can be apparently a contradiction, since serpentinization should occur under low to moderate oxidizing conditions, whereas steatitic rocks are formed under strong oxidizing conditions, usually with high CO_2 activity. An explanation for this

Table 4. Electron microprobe analyses of magnetite in serpentinites and steatitic rocks from northeastern Portugal.

	Serpentinite	Steatitic rock	
	Donai	Sete Fontes	Soeira/ Pena Maquieira
SiO_2	0.22	0.01	0.06
TiO_2	0.01	0.01	0.02
Cr_2O_3	0.09	0.27	0.93
Fe_2O_3	68.82	69.41	68.98
FeO	30.84	30.91	31.17
MnO	0.02	-	-
MgO	0.33	0.02	0.03
ZnO	0.13	n. a.	n. a.
NiO	-	0.26	0.38
CaO	0.00	0.17	0.05
Total	100.46	101.06	101.62
Si	0.068	0.004	0.018
Cr	0.022	0.066	0.222
Fe^{3+}	15.834	15.922	15.732
Ti	0.004	0.002	0.005
S	15.93	15.99	15.98
Mg	0.153	0.009	0.013
Fe^{2+}	7.885	7.879	7.900
Zn	0.029	-	-
Ni	-	0.064	0.093
Mn	0.004	-	-
Ca	0.002	0.055	0.017
Σ	8.07	8.01	8.02

Fe_2O_3 and FeO were calculated according to the method of Droop (1987); - : not detected; n. a.– not analysed. Number of cations on the basis of 32 atoms of oxygen.
Analyst: R.J.S. Teixeira.

situation can be related to the occurrence of hydrothermal metamorphic reactions between the magmatic spinels and the surrounding post-serpentinization silicate matrix, rather than with a direct interaction with high temperature (> 400 ºC) MgO- and SiO_2-rich fluids (Kimball, 1990; Mellini et al., 2005). The formation of chlorite aureoles through spinel alteration could imply, in a first moment, the replacement of the primitive spinel by a multiphase ferrian chromite rim, which can consist in a lizardite, chlorite and Cr-magnetite intergrown (Mellini et al., 2005). In a second stage, the outer serpentine would be progressively transformed, due to the diffusion of Al and Mg, into chlorite or to a disordered chlorite/lizardite intergrowth (Mellini et al., 2005). The formation of chlorite aureoles has also been described and explained by other investigators, such as Bliss and MacLean (1975), Pinsent and Hirst (1977), Boukili et al. (1984), Whittaker and Watkinson (1984), Gianfagna et al. (1992), Leblanc and Nicolas (1992), Garuti et al. (2007) and González-Jiménez et al. (2009). The formation of chlorite aureoles through the chromian spinel alteration could also explain the progressive decrease in Al_2O_3 during the retrograde evolution of the serpentinite of Donai (Teixeira et al., 2002).

Concerning the magnetite with composition close to the ideal formula, two considerations can be made: 1) the magnetite minute crystals located in the rims of the mesh cells in the Figure 6d should be produced by a low temperature alteration process (retrograde metamorphism) of peridotites. In contrast, magnetite reported in Figure 6e shows clear replacement textures, probably formed by oxidation of the associated sulphides (pyrrhotite and pentlandite).

Furthermore, the following equation proposed by Klein et al. (2009), Olivine + H_2O → Serpentine + Brucite + Magnetite + H_2, shows, as mentioned before, that serpentinization is a highly reducing process because the alteration of olivine by aqueous fluids produces significant amounts of hydrogen that strongly decreases the fO_2 and fS_2 values by its reaction with O_2 to form H_2O and with S_2 to form H_2S. Such environment contributes to form sulphides impoverished in S and Ni-Fe alloys (Eckstrand, 1975; Frost, 1985; Klein and Bach, 2009). In fact, all the studied serpentinites contain pentlandite, but at Donai pyrrhotite is also found, forming aggregates with

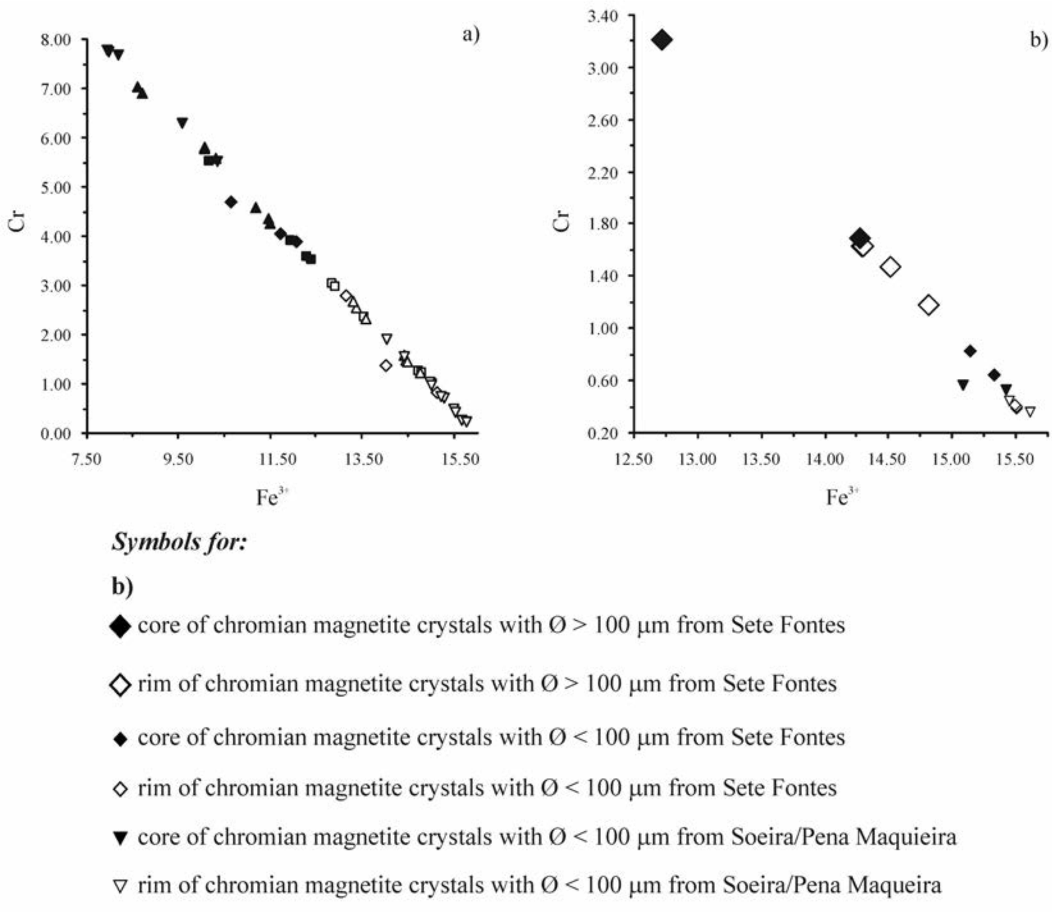

Figure 10. Cr versus Fe^{3+} for chromian magnetite from Sete Fontes and Soeira/Pena Maquieira. a) crystals with a diameter (Ø) > 150 mm; b) crystals with a Ø < 150 mm in steatitic rocks. Symbols for Figure 10a as in Figures 8b, c.

pentlandite (Figures 6a, e). The production of H_2 during serpentinization should stop as soon as olivine is totally altered. However, the continuous addition of aqueous fluids (especially if they carry some CO_2) could rise up both fO_2 and fS_2 promoting the formation of S-rich sulphides and carbonates (Khalil and El-Makky, 2009), such as breunnerite and dolomite that may occur in the studied serpentinites. In contrast, the formation of steatitic rocks requires a high activity of CO_2 and high fO_2. The fS_2 should have been high too as evidenced by the sulphide assemblage made up of pentlandite in association with millerite, pyrite and siegenite.

Conclusions

1) The compositions of Cr-rich hercynite and aluminian chromite crystals of serpentinite and steatitic rock from Donai were probably

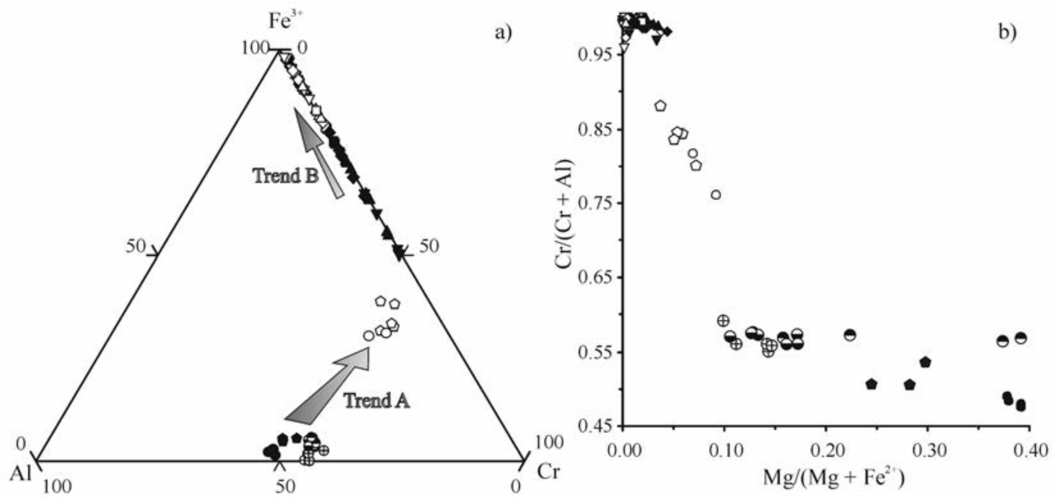

Figure 11. a) Compositions of spinels from Bragança massif plotted on Fe^{3+}-Al-Cr ternary diagram; the arrows indicate the alteration trends A and B. b) Cr/(Cr + Al) versus Mg/(Mg + Fe^{2+}) diagram for chromian spinels from serpentinites and steatitic rocks from Bragança massif. Symbols as in Figure 8.

modified due to post-serpentisation hydrothermal metamorphic reactions between these spinels and the surrounding serpentine matrix, rather than to a direct interaction with the serpentinization fluids. These subsequent interactions should have occurred under stronger oxidizing conditions, promoting the enrichment in Fe^{3+} and the impoverishment in Mg, Al and Co and, consequently, the formation of ferrian chromite rims.

2) The rare unzoned aluminian chromite from Donai chloritite is the richest in Zn. It was stable and apparently unaltered during the chloritisation process that affected an igneous protolith probably of mafic nature.

3) During the late asbestisation process, the alteration of the rare aluminian chromite crystals that may occur in tremolite asbestos from Donai is shown by a decrease in Mg and an increase in Fe^{2+} from core to rim. This alteration trend is not accompanied by a Fe^{3+} enrichment, which may indicate that tremolite could buffer the fO_2 in this type of rock.

4) The ultramafic rocks from Sete Fontes and Soeira/Pena Maquieira were mostly steatised, and chromian magnetite crystals were decomposed due to the dissolution of Al, Cr, Mg and Zn under strong oxidizing conditions, usually with high CO_2 activity. The chromian magnetite rims are richer in Fe^{3+}, Fe^{2+} and Ni than the respective cores.

5) The chromian spinel crystals with Cr/(Cr + Al) lower than 0.60 are usually surrounded by chlorite aureoles, whereas those chromian spinel crystals with Cr/(Cr + Al) greater than 0.95 just show chromian magnetite rims. The chlorite aureoles were probably formed due to the diffusion of Al and Mg from chromian spinel to the surrounding serpentine.

6) Magnetite was found in Donai serpentinite and in steatitic rocks from Sete Fontes and Soeira/Pena Maquieira and has a composition close to the ideal formula, but small contents of Cr and Mg, Ni, Mn, Ca replace Fe^{3+} and Fe^{2+}, respectively. The

magnetite of mesh rims was produced during the retrograde metamorphism that affected the initial peridotites. On the other hand, the magnetite replacing sulphides was probably formed by an oxidation process.

Acknowledgements

We are grateful to Prof. M.R. Machado Leite, Dr. J.M. Farinha Ramos and Mr. F.A.P. Santos for the use of electron microprobe at the Laboratório Nacional de Energia e Geologia, São Mamede de Infesta, Portugal. Thanks are also due to Prof. B.J. Wood for providing access to the EUGF-Bristol facility, contract ERBFMGECT 980128, where R.J.S. Teixeira used the electron microprobe of the Department of Earth Sciences, University of Bristol, United Kingdom. Dr. Stuart Kearns is thanked for his skilled assistance during the electron microprobe session. R.J.S. Teixeira also thanks to Álvaro Miranda, Nelson Pinto, Simão Botelho and Tito Azevedo for their help in field and laboratory works. This research was carried out in the program of Geosciences Centre, University of Coimbra, Portugal. This paper benefited from the very helpful comments of Prof. Antonio Gianfagna (Editor) and two anonymous reviewers.

References

Angeli N., Fleet M.E., Thibault Y. and Candia M.A.F. (2001) - Metamorphism and PGE-Au content of chromitite from the Ipanema mafic/ultramafic Complex, Minas Gerais, Brazil. *Mineralogy and Petrology*, 71, 173-194.

Barnes S.J. (2000) - Chromites in komatiites, II, Modification during greenschist to mid-amphibolite facies metamorphism. *Journal of Petrology*, 41, 387-409.

Barnes S.J. and Roeder P.L. (2001) - The range of spinel compositions in terrestrial mafic and ultramafic rocks. *Journal of Petrology*, 42, 2279-2302.

Beeson M.H. and Jackson E.D. (1969) - Chemical composition of altered chromite from the Stillwater Complex, Montana. *American Mineralogist*, 54, 1084-1100.

Bliss N.W. and MacLean W.H. (1975) - The paragenesis of zoned chromite from central Manitoba. *Geochimica et Cosmochimica Acta*, 39, 973-990.

Boukili H., Novikoff A., França J. (1984) - Mineralogie et géochimie des chlorites et hydroxycarbonates chromitifères de Campo Formoso, Bahia, Brésil. *Cah. O.R.S.T.O.M. sér. Géol*., XIV/2, 141-152.

Bridges J.C., Prichard H.M., Neary C.R. and Meireles C.A. (1993) - Platinum-group element mineralization in chromite-rich rocks of Bragança massif, northern Portugal. *Transactions of the Institution of Mining and Metallurgy*, 102, B103-B113.

Burkhard D.J.M. (1993) - Accessory chromium spinels: their coexistence and alteration in serpentinites. *Geochimica et Cosmochimica Acta*, 57, 1297-1306.

Cotelo Neiva J.M. (1948) - Rochas e minérios da região Bragança - Vinhais. *Serviço de Fomento Mineiro*, 14, 1-251.

Deer W.A., Howie R.A. and Zussman J. (1992) - An introduction to the rock-forming minerals, 2nd *Ed.*, Longman Scientific & Technical, New York, U.S.A., 695 pp.

Droop G.T.R. (1987) - A general equation for estimating Fe^{3+} concentrations in ferromagnesian silicates and oxides from microprobe analyses, using stoichiometric criteria. *Mineralogical Magazine*, 51, 431-435.

Eckstrand O.R. (1975) - The Dumont serpentinite: a model for control of nickeliferous opaque mineral assemblages by alteration reactions in ultramafic rocks. *Economic Geology*, 70, 183-201.

Frost B.R. (1985) - On the stability of sulfides, oxides and native metals in serpentinite. *Journal of Petrology*, 26, 31-63.

Garuti G., Proenza J.A. and Zaccarini F. (2007) - Distribution and mineralogy of platinum-group elements in altered chromitites of the Campo Formoso layered intrusion (Bahia State, Brazil): Control by magmatic and hydrothermal processes. *Mineralogy and Petrology*, 89, 159-188.

Gianfagna A., Grubessi O. and Massera S. (1992) - Cr-rich-spinel chemistry of the serpentinites from the island of Elba, Tuscany, Italy: note I. *Atti della Società Toscana di Scienze Naturali Memorie*, 99,175-194.

González-Jiménez J.M., Kerestedjian T., Proenza J.A. and Gervilla F. (2009) - Metamorphism on chromite ores from the Dobromirtsi ultramafic massif, Rhodope Mountains (SE Bulgaria). *Geologica Acta*, 7, 413-429.

Haggerty S.E. (1976) - Opaque minerals in terrestrial igneous rocks. In: Oxide Minerals (Rumble III, D., ed.). *Reviews in Mineralogy*, 3, 101-300.

Izquierdo B.G., Lunar R., Capote R. and Moreno T. (2002) - Mobilization of Al-Cr in spinel during deformation of ultramafic rocks from Cabo Ortegal and Bragança Complexes, NW Iberian Peninsula (Spain and Portugal). *Programme with abstracts - 18th general meeting of the International Mineralogical Association*, 219-220.

Karipi S., Tsikouras B., Hatzipanagiotou K. and Grammatikopoulos T.A. (2007) - Petrogenetic significance of spinel-group minerals from the ultramafic rocks of the Iti and Kallidromon ophiolites (Central Greece). *Lithos*, 99, 136-149.

Khalil K.I. and El-Makky A.M. (2009) - Alteration mechanisms of chromian-spinel during serpentinization at Wadi Sifein Area, Eastern Desert, Egypt. *Resource Geology*, 59, 194-211.

Kimball K.L. (1990) - Effects of hydrothermal alteration on the composition of chromian spinels. *Contributions to Mineralogy and Petrology*, 105, 337-346.

Klein F. and Bach W. (2009) - Fe-Ni-Co-O-S phase relations in peridotite-seawater interactions. *Journal of Petrology*, 50, 37-59.

Klein F., Bach W., Jöns N., McCollom T., Moskowitz B. and Berquo T. (2009) - Iron partitioning and hydrogen generation during serpentinization of abyssal peridotites from 15°N on the Mid-Atlantic Ridge. *Geochimica et Cosmochimica Acta*, 73, 6868-6893.

Leblanc M. and Nicolas A. (1992) - Ophiolitic chromitites. *International Geology Review*, 34, 653-686.

Marques F.O., Ribeiro A. and Munhá J.M. (1996) - Geodynamic evolution of the continental allochthonous terranes (CAT) of the Bragança Nappe Complex, NE Portugal. *Tectonics*, 15, 747-762.

Meireles C., Santos J., Pereira E. and Ribeiro. A. (1999) - Carta Geológica de Portugal à escala 1:50 000 (Folha 3-D, Espinhosela). Serviços Geológicos de Portugal.

Mellini M., Rumori C. and Viti C. (2005) - Hydrothermally reset magmatic spinels in retrograde serpentinites: formation of "ferritchromit" rims and chlorite aureoles. *Contributions to Mineralogy and Petrology*, 149, 266-275.

Mondal S.K., Ripley E.M., Lib C. and Frei R. (2006) - The genesis of Archaean chromitites from the Nuasahi and Sukinda massifs in the Singhbhum Craton, India. *Precambrian Research*, 148, 45-66.

Munhá J.M., Ribeiro A. and Ribeiro M.L. (1984) - Blueschists in the Iberian Variscan chain (Trás-os-Montes, NE Portugal). *Comunicações dos Serviços Geológicos de Portugal*, 70, 31-53.

O' Hanley D.S. (1996) - Serpentinites: Records of tectonic and petrological history. Oxford University Press, New York, U.S.A., 277 pp.

Peltonen P. (1995) - Crystallization and re-equilibration of zoned chromite in ultramafic cumulates, Vammala Ni-Belt, southwestern Finland. *The Canadian Mineralogist*, 33, 521-535.

Pinsent R.H. and Hirst D.M. (1977) - The metamorphism of the Blue River ultramafic body, Cassiar, British Columbia, Canada. *Journal of Petrology*, 18, 567-594.

Pooley G.D. (2004). Secondary and backscattered electron imaging of weathered chromian spinel. *Scanning*, 26, 240-249.

Proenza J., Solé J. and Melgarejo J.C. (1999) - Uvarovite in podiform chromitite: The Moa-Baracoa ophiolitic massif, Cuba. *Canadian Mineralogist*, 37, 679-690.

Ramos J.F., Moura A.C., Grade J. and Amarante M. (1989) - Estudo químico-mineralógico e de beneficiação de talcos de Bragança - Vinhais (NE de Portugal). *Estudos, Notas e Trabalhos*, 31, 29-77.

Ribeiro A. (1974) - Contribution à l´étude tectonique de Trás-os-Montes Oriental. Serviços Geológicos de Portugal (Memória nº 24 - Nova Série), 168 pp.

Ribeiro A., Pereira E. and Dias R. (1990) - Allochtonous sequences: Structure in the Northwest of the Iberian Peninsula. In: Pre-Mesozoic Geology of Iberia (Dallmeyer R.D. and Martinez Garcia E., eds.). Berlin Heidelberg, Springer-Verlag, 220-236.

Sansone M.T.C., Prosser G, Rizzo G. and Tartarotti P. (2012) - Spinel-peridotites of the Frido Unit ophiolites (Southern Apennine-Italy): evidence for oceanic evolution. *Periodico di Mineralogia*, 81, 35-59.

Shen P., Hwang S., Chu H. and Jeng R. (1988) - STEM study of "ferritchromit" from the Heng-Chun chromitite. *American Mineralogist*, 73, 383-388.

Stevens R.E. (1944) - Composition of some chromites of western hemisphere. *American Mineralogist*, 29, 1-34.

Teixeira R.J.S. (2000) - Serpentina, asbesto e talco: Impacte ambiental das suas explorações no Nordeste de Portugal. Unpublished M. Sc. Thesis, University of Coimbra, Portugal, 247 pp.

Teixeira R.J.S., Neiva A.M.R. and Gomes M.E.P. (2002) - Geochemistry of serpentinites and steatitic rocks from Bragança, northeastern Portugal. Programme with abstracts - 18th general meeting of the International Mineralogical Association: 225-226.

Ulmer G.C. (1974) - Alteration of chromite during serpentinization in the Pennsylvania-Maryland district. *American Mineralogist*, 59, 1236-1241.

Vilela de Matos A., Alves P.H. and Coke C. (1990) - Valorização das jazidas de talco - COMITAL: Relatório final - Acções preparatórias do programa integrado de desenvolvimento regional de Trás-os-Montes. Unpublished Report, University of Trás-os-Montes e Alto Douro, Vila Real, Portugal.

Whittaker P.J. and Watkinson D.H. (1984) - Genesis of chromitite from the Mitchel range, central British Columbia. *Canadian Mineralogist*, 22, 161-172.

Wylie A.G, Candela P.A., and Burke T.M. (1987) - Compositional zoning in unusual Zn-rich chromite from Sykesville district of Maryland and its bearing on the origin of “ferrichromit”. *American Mineralogist*, 72, 413-422.

Zakrevskaya O.Y., Simakin A.G. and Salova T.P. (2009) - *Electronic Scientific Information Journal “Vestnik Otdelenia nauk o Zemle RAN”*, 1 (27), 1-4.

Submitted, May 2012 - Accepted, July 2012